

Article

# Novel Group of AChE Reactivators—Synthesis, In Vitro Reactivation and Molecular Docking Study

David Malinak<sup>1,2</sup>, Eugenie Nepovimova<sup>1</sup>, Daniel Jun<sup>2,3</sup>, Kamil Musilek<sup>1,2,\*</sup>  and Kamil Kuca<sup>1,\*</sup> 

<sup>1</sup> Department of Chemistry, Faculty of Science, University of Hradec Kralove, Rokitanskeho 62, 500 03 Hradec Kralove, Czech Republic; david.malinak@uhk.cz (D.M.); eugenie.nepovimova@uhk.cz (E.N.)

<sup>2</sup> University Hospital in Hradec Kralove, Sokolska 581, 500 05 Hradec Kralove, Czech Republic; daniel.jun@unob.cz

<sup>3</sup> Department of Toxicology and Military Pharmacy, Faculty of Military Health Sciences, University of Defence, Trebesska 1575, 500 01 Hradec Kralove, Czech Republic

\* Correspondence: kamil.musilek@uhk.cz (K.M.); kamil.kuca@uhk.cz (K.K.); Tel.: +420-493-332-780 (K.K.)

Received: 15 August 2018; Accepted: 5 September 2018; Published: 7 September 2018



**Abstract:** The acetylcholinesterase (AChE) reactivators (e.g., obidoxime, asoxime) became an essential part of organophosphorus (OP) poisoning treatment, together with atropine and diazepam. They are referred to as a causal treatment of OP poisoning, because they are able to split the OP moiety from AChE active site and thus renew its function. In this approach, fifteen novel AChE reactivators were determined. Their molecular design originated from former K-oxime compounds K048 and K074 with remaining oxime part of the molecule and modified part with heteroarenium moiety. The novel compounds were prepared, evaluated in vitro on human AChE (*HssAChE*) inhibited by tabun, paraoxon, methylparaoxon or DFP and compared to commercial *HssAChE* reactivators (pralidoxime, methoxime, trimedoxime, obidoxime, asoxime) or previously prepared compounds (K048, K074, K075, K203). Some of presented oxime reactivators showed promising ability to reactivate *HssAChE* comparable or higher than the used standards. The molecular modelling study was performed with one compound that presented the ability to reactivate GA-inhibited *HssAChE*. The SAR features concerning the heteroarenium part of the reactivator's molecule are described.

**Keywords:** organophosphate; acetylcholinesterase; reactivation; oxime; in vitro; molecular docking

## 1. Introduction

Organophosphorus agents (OP) are among the most toxic compounds developed by humans. They were originally discovered as pesticides (e.g., paraoxon, methylparaoxon; Figure 1), but they were further introduced as nerve agents (e.g., tabun, sarin, soman, VX; Figure 1), with highly lethal effects [1]. Some OPs are also utilized as industrial agents (e.g., flame retardants). Their mechanism of action is based on the irreversible inhibition of cholinesterases [2]. The toxic effect is caused by inhibition of acetylcholinesterase (AChE), while inhibited butyrylcholinesterase (BChE) takes part as an OP bioscavenger [3]. The inhibited AChE cannot fulfil its native function of degrading the neurotransmitter acetylcholine. Thus, acetylcholine is accumulated in the synapses, causing permanent stimulation of the cholinergic (muscarinic or nicotinic) receptors. For this reason, cholinergic symptoms (e.g., miosis, salivation, lacrimation, breath depression) occur that may worsen to cholinergic crisis or death from the malfunction of breathing muscles and the depression of the breathing center in the central nervous system [4].

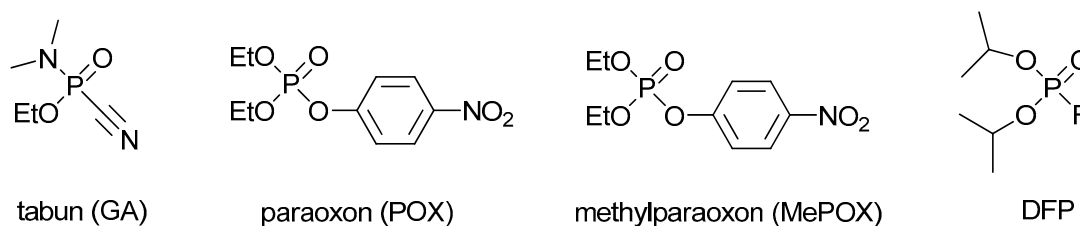


Figure 1. Selected organophosphorus compounds.

OP intoxication is usually managed using two treatment strategies. The first pre-treatment strategy for first responders (e.g., soldiers, medical staff) consists in the protection of the organism against OP attack. Pre-treatment can be performed using reversible AChE inhibitors (e.g., pyridostigmine chloride), stoichiometric scavengers (e.g., recombinant BChE) or catalytic bioscavengers (e.g., phosphotriesterase, paraoxonase) [5,6]. The second post-treatment strategy consists of managing already-OP-intoxicated organisms. The symptomatic post-treatment is focused on the amelioration of the OP intoxication symptoms [2]. Atropine (parasympatholytic drug) and diazepam (anticonvulsive drug), connected to supportive care, are usually used for this purpose [4]. The causal post-treatment is provided by oxime reactivators (e.g., pralidoxime, asoxime, obidoxime, trimedoxime, methoxime; 1–5; Figure 2) via nucleophilic attack of the oximate towards the OP-AChE complex [7]. Such drugs are able to split the OP moiety from the AChE active site and restore its native function. The reactivation depends on many factors, e.g., OP dose, type of reactivator and its potency against certain OP, delay of reactivation treatment [8]. In fact, there is not a single reactivator available for a broad variety of OP compounds. The treatment is made even more complicated by the process of aging [9]. The OP moiety bound to the cholinesterase active site is further coordinated via loss of one ester moiety (*O*-dealkylation). Negatively charged oxygen appears, and the nucleophilic oxime reactivator is further ineffective. The aging process is well documented for nerve agents (over a time scale from minutes to hours), but some pesticides (e.g., methamidophos) may also be dealkylated in a similar manner [10].

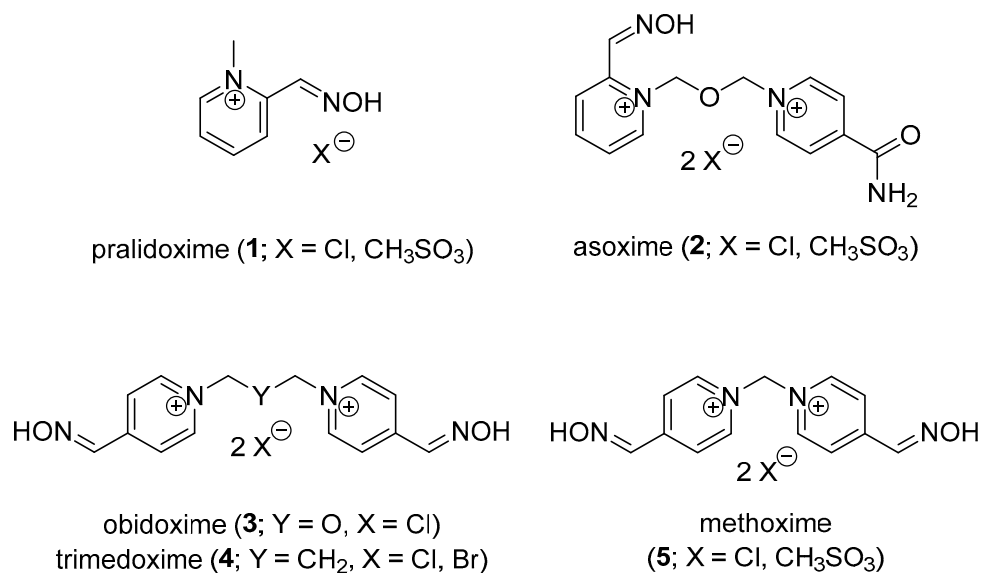


Figure 2. Commercially available AChE reactivators.

Though the asoxime (2) was formerly found to be the most broad-spectrum oxime reactivator for nerve agent poisonings, it is not able to counteract, e.g., tabun or OP pesticide intoxication [11]. Thus, many scientific teams are trying to develop reactivators for nerve agent-inhibited AChE and/or OP pesticide poisoning. Recently, both quaternary and non-quaternary AChE reactivators have been considered for possible management of OP intoxication, including tabun exposure [12,13].

## 2. Design and Synthesis Mono-Oxime Bispyridinium Reactivators

The development of mono-oxime AChE reactivators with tetramethylene linker is described in this paper. The design of this series of compounds originated from the former series of oxime reactivators with (*E*)-but-2-en-1,4-diyl (6–7) and but-1,4-diyl (8–9) linkage, which showed some promising compounds for further study by *in vitro* and *in vivo* experiments (Figure 3) [14,15].

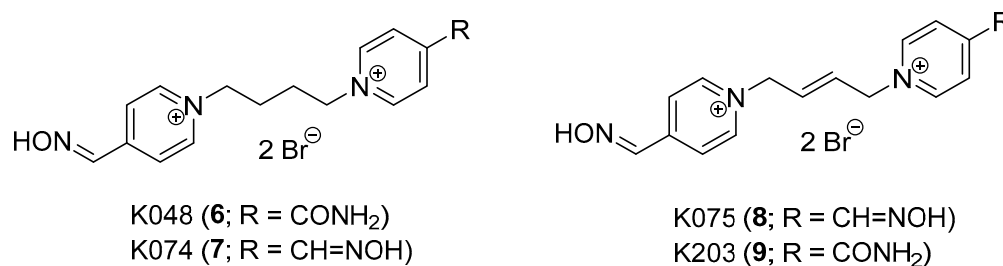


Figure 3. Promising formerly developed AChE reactivators.

The nerve agent tabun (GA) remains the main OP of reactivation interest, followed by the selected OP pesticides. The previous structural findings showed that mono-oxime bispyridinium compounds (6, 9) may have similar reactivation abilities against tabun-inhibited AChE as the known bis-oximes (3–4) [16,17]. Furthermore, the connection linkage at a length of 3–4 C-C bonds between two pyridinium moieties was considered to be optimal for GA reactivation [18]. For this reason, prop-1,3-diyl, but-1,4-diyl and (*E*)-but-2-en-1,4-diyl linkers were previously used [14,15]. The but-1,4-diyl linkage was the spacer that best fulfilled the found length criterion. Additionally, the bis-oxime compound with but-1,4-diyl linker (7) was previously found to be a potent reactivator of GA-inhibited AChE, although it resulted in increased toxicity during the *in vivo* studies [19,20].

For the above-mentioned reasons, bisquaternary mono-oxime compounds with but-1,4-diyl linkage and varying second pyridinium ring or moiety on the second pyridinium ring were designed (10–24; Figure 4).

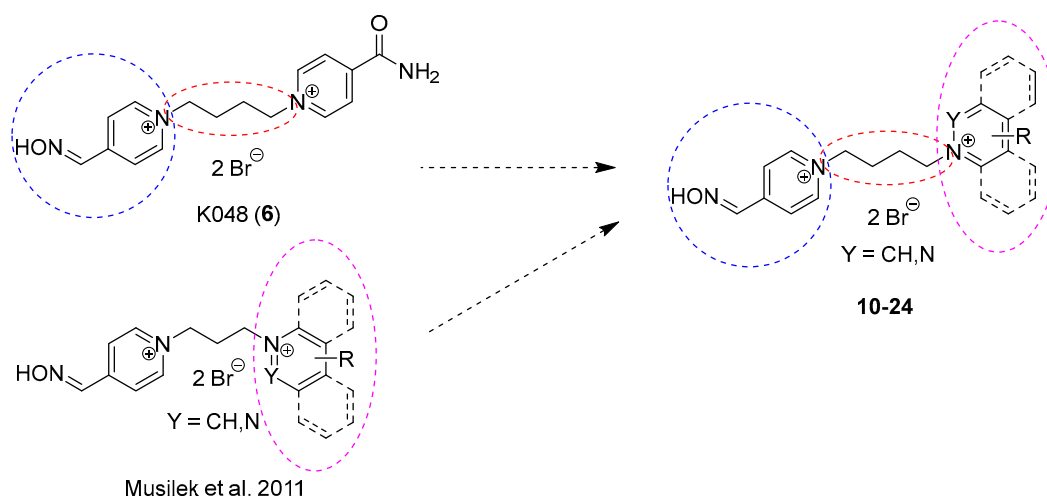
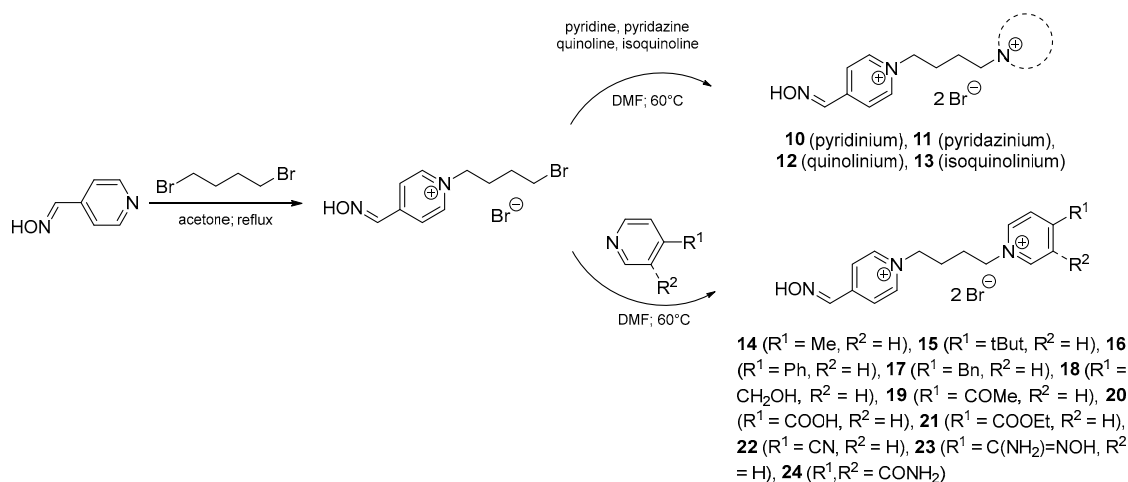


Figure 4. Design of bisquaternary mono-oxime reactivators with but-1,4-diyl linkage.

This second moiety was designed in the 4-position of the second pyridinium ring to allow the reactivator molecule to penetrate into the narrow AChE active site. The non-oxime moieties were chosen as representatives of hydrophilic (e.g., hydroxymethyl, methylcarbonyl, carboxyl, ethylcarboxyl, nitrile, amidoxime; 18–24) and hydrophobic (e.g., methyl, tert-butyl, phenyl, benzyl; 14–17) nature, or the whole pyridinium moiety was replaced by another heteroarene ring (e.g., pyridazinium, quinolinium, isoquinolinium; 10–13). The selected changes were designed to establish more possible

interactions between reactivator and AChE, whether the  $\pi$ -cationic,  $\pi$ - $\pi$  or hydrogen bonding interactions were the most common ones [21].

The mono-oxime reactivators with tetramethylene linker were synthesized via a standard 2-step strategy (Scheme 1) [15]. The monoquaternary compound were prepared in 5 molar excess of the alkylating agent (1,4-dibromobutane). The monoquaternary compound was further separated from the side bisquaternary side product by crystallization from acetonitrile (MeCN), where the bisquaternary side product was almost insoluble. Secondly, the synthesis of mono-oxime reactivator was completed by the addition of appropriate heterocyclic agent (1.5 molar excess). The crystallization of MeCN was used again to give non-soluble bisquaternary reactivator (**10–24**) in a satisfactory purity and yield.



**Scheme 1.** Synthesis of mono-oxime reactivators with tetramethylene linker.

### 3. Results and Discussion

#### 3.1. HssAChE Reactivation Results

The reactivation experiments were performed on human recombinant AChE (*HssAChE*) inhibited by tabun (GA), paraoxon (POX), methylparaoxon (MePOX) or diisopropylfluorophosphate (DFP) using the standard Ellman protocol [22]. GA was selected as the nerve agent of main interest. The chosen OP pesticides (POX, MePOX) and the mimic agent (DFP) were used, as they are distinct members of the OP family with remaining dimethyl-(MePOX), diethyl-(POX) or diisopropyl-(DFP) scaffolds after AChE inhibition. The reactivation results for all tested compounds are listed in Table 1.

The reactivation results for tabun-inhibited *HssAChE* showed extensive differences, even in the group of commercial and known compounds [23]. Among these, pralidoxime (**1**), asoxime (**2**) and methoxime (**5**) showed poor reactivation ability [23]. On the other hand, obidoxime (**3**), trimedoxime (**4**) and compounds **6–9** displayed increased reactivation, with the best results being obtained for K203 (**9**; 48%) at 100  $\mu\text{M}$  and K074 (**7**; 25%) at 10  $\mu\text{M}$  concentration. Taken together with toxicity issues, some previously known AChE reactivators (e.g., **9**) have improved reactivation ability towards tabun both in vitro and in vivo [24]. The newly prepared compounds were prepared with the idea of improved tabun-inhibited *HssAChE* reactivation. However, this objective was not fulfilled on the basis of the in vitro data for both tested concentrations, with the exception of compound **23**. Reactivator **23** (13%) showed better results than commercial compound **3** (8%) at 10  $\mu\text{M}$  concentration, which tends to be attainable in blood after possible in vivo administration, but its activity was found to be worse than previously known compounds **4** (17%), **7–9** (25%, 18%, 21%) [25].

**Table 1.** Reactivation results of commercial, formerly published and newly prepared AChE reactivators.

Compound	Non-Reactivating Moiety	GA- <i>HssAChE</i> Reactivation (% $\pm$ SD)		POX- <i>HssAChE</i> Reactivation (% $\pm$ SD)		MePOX- <i>HssAChE</i> Reactivation (% $\pm$ SD)		DFP- <i>HssAChE</i> Reactivation (% $\pm$ SD)		<i>HssAChE</i> IC <sub>50</sub> $\pm$ SD
		100 $\mu$ M	10 $\mu$ M	100 $\mu$ M	10 $\mu$ M	100 $\mu$ M	10 $\mu$ M	100 $\mu$ M	10 $\mu$ M	
1 (2-PAM)	-	3.3 $\pm$ 0.5	2.4 $\pm$ 0.2	10.7 $\pm$ 0.3	2.1 $\pm$ 0.1	30.2 $\pm$ 0.3	22.4 $\pm$ 0.7	1.3 $\pm$ 0.6	0.1 $\pm$ 0.4	878 $\pm$ 171
2 (HI-6)	CONH <sub>2</sub>	0.9 $\pm$ 0.6	0.8 $\pm$ 0.3	6.2 $\pm$ 0.6	1.7 $\pm$ 0.1	13.6 $\pm$ 0.2	17.9 $\pm$ 0.4	0.7 $\pm$ 0.1	1.4 $\pm$ 0.1	203 $\pm$ 39
3 (obidoxime)	CH=NOH	15.1 $\pm$ 0.9	7.9 $\pm$ 0.5	59.7 $\pm$ 1.0	22.4 $\pm$ 0.4	61.7 $\pm$ 0.3	45.3 $\pm$ 0.9	7.6 $\pm$ 0.7	3.3 $\pm$ 0.4	577 $\pm$ 113
4 (trimedoxime)	CH=NOH	31.5 $\pm$ 1.2	16.9 $\pm$ 0.2	44.3 $\pm$ 0.6	22.5 $\pm$ 1.3	51.4 $\pm$ 0.9	59.5 $\pm$ 0.7	10.0 $\pm$ 0.5	2.7 $\pm$ 0.3	167 $\pm$ 33
5 (methoxime)	CH=NOH	2.9 $\pm$ 0.01	2.1 $\pm$ 0.5	16.1 $\pm$ 0.5	1.8 $\pm$ 0.3	14.2 $\pm$ 0.1	14.3 $\pm$ 0.2	2.4 $\pm$ 0.1	0.6 $\pm$ 0.3	2010 $\pm$ 391
6 (K048)	CONH <sub>2</sub>	27.4 $\pm$ 1.1	10.0 $\pm$ 0.6	25.7 $\pm$ 0.7	12.5 $\pm$ 0.2	54.4 $\pm$ 0.9	29.1 $\pm$ 0.4	3.8 $\pm$ 0.1	1.4 $\pm$ 0.1	349 $\pm$ 68
7 (K074)	CH=NOH	32.1 $\pm$ 0.6	24.6 $\pm$ 0.2	31.1 $\pm$ 0.4	13.9 $\pm$ 0.8	17.9 $\pm$ 0.1	21.2 $\pm$ 0.4	1.4 $\pm$ 0.5	1.4 $\pm$ 0.2	29 $\pm$ 6
8 (K075)	CH=NOH	19.5 $\pm$ 1.0	18.1 $\pm$ 0.2	28.5 $\pm$ 1.1	14.1 $\pm$ 0.3	19.2 $\pm$ 0.9	22.8 $\pm$ 0.2	1.1 $\pm$ 0.3	1.5 $\pm$ 0.2	80 $\pm$ 16
9 (K203)	CONH <sub>2</sub>	48.1 $\pm$ 1.5	21.2 $\pm$ 0.3	39.3 $\pm$ 0.4	13.1 $\pm$ 0.4	55.9 $\pm$ 0.5	41.1 $\pm$ 0.1	4.4 $\pm$ 0.1	2.1 $\pm$ 0.4	566 $\pm$ 110
10	pyridinium	3.9 $\pm$ 0.1	4.5 $\pm$ 0.3	16.6 $\pm$ 1.0	3.5 $\pm$ 0.3	14.3 $\pm$ 0.8	13.2 $\pm$ 0.1	2.4 $\pm$ 0.5	0.4 $\pm$ 0.3	-
11	pyridazinium	1.5 $\pm$ 0.5	4.1 $\pm$ 0.2	6.3 $\pm$ 0.8	3.0 $\pm$ 0.3	7.1 $\pm$ 0.7	11.8 $\pm$ 0.4	1.2 $\pm$ 0.7	1.0 $\pm$ 0.4	-
12	quinolinium	0.6 $\pm$ 0.4	3.1 $\pm$ 0.3	0.6 $\pm$ 0.5	2.0 $\pm$ 0.1	2.2 $\pm$ 0.5	8.6 $\pm$ 0.4	0.2 $\pm$ 1.0	0.8 $\pm$ 0.2	-
13	isoquinolinium	3.5 $\pm$ 0.7	6.0 $\pm$ 0.2	9.1 $\pm$ 0.3	8.7 $\pm$ 0.3	8.2 $\pm$ 0.8	16.9 $\pm$ 0.4	0.7 $\pm$ 0.2	1.1 $\pm$ 0.2	-
14	Me	3.4 $\pm$ 0.4	6.3 $\pm$ 0.3	24.5 $\pm$ 0.3	7.6 $\pm$ 0.6	9.5 $\pm$ 0.5	9.4 $\pm$ 0.2	1.1 $\pm$ 0.4	0.8 $\pm$ 0.3	-
15	tBut	1.7 $\pm$ 0.4	3.9 $\pm$ 0.3	18.7 $\pm$ 0.2	58.7 $\pm$ 4.0	4.0 $\pm$ 0.5	7.6 $\pm$ 0.5	1.7 $\pm$ 0.5	0.8 $\pm$ 0.3	24 $\pm$ 6
16	Ph	0.7 $\pm$ 0.4	3.5 $\pm$ 0.3	6.9 $\pm$ 0.4	8.9 $\pm$ 0.5	1.7 $\pm$ 0.3	6.2 $\pm$ 0.4	0.7 $\pm$ 0.2	1.0 $\pm$ 0.3	6 $\pm$ 1
17	Bn	0.3 $\pm$ 0.2	1.9 $\pm$ 0.6	1.2 $\pm$ 0.1	4.7 $\pm$ 0.3	0.0 $\pm$ 0.1	3.8 $\pm$ 0.4	0.0 $\pm$ 0.5	0.8 $\pm$ 0.2	-
18	CH <sub>2</sub> OH	2.6 $\pm$ 0.3	4.0 $\pm$ 0.3	20.6 $\pm$ 0.1	8.0 $\pm$ 0.1	6.7 $\pm$ 0.3	8.1 $\pm$ 0.3	3.8 $\pm$ 1.0	1.4 $\pm$ 0.4	-
19	COMe	1.7 $\pm$ 0.3	3.1 $\pm$ 0.1	11.9 $\pm$ 1.0	3.9 $\pm$ 0.3	5.2 $\pm$ 0.4	7.5 $\pm$ 0.1	1.5 $\pm$ 0.3	1.0 $\pm$ 0.2	-
20	COOH	3.3 $\pm$ 0.5	6.2 $\pm$ 0.3	14.5 $\pm$ 0.6	4.2 $\pm$ 0.4	9.5 $\pm$ 0.3	8.8 $\pm$ 0.4	1.1 $\pm$ 0.5	0.4 $\pm$ 0.1	-
21	COOEt	1.7 $\pm$ 0.5	4.1 $\pm$ 0.2	7.1 $\pm$ 0.7	4.0 $\pm$ 0.6	3.8 $\pm$ 0.4	7.2 $\pm$ 0.2	0.8 $\pm$ 0.3	1.1 $\pm$ 0.2	-
22	CN	3.6 $\pm$ 0.4	5.2 $\pm$ 0.2	10.1 $\pm$ 0.8	42.6 $\pm$ 0.1	11.1 $\pm$ 0.1	13.8 $\pm$ 0.3	1.7 $\pm$ 0.5	0.4 $\pm$ 0.2	45 $\pm$ 9
23	C(NH <sub>2</sub> )=NOH	12.8 $\pm$ 0.9	13.1 $\pm$ 0.4	19.1 $\pm$ 0.8	7.4 $\pm$ 0.3	20.2 $\pm$ 1.0	20.7 $\pm$ 0.4	3.1 $\pm$ 0.8	2.0 $\pm$ 0.2	90 $\pm$ 17
24	3,4-CONH <sub>2</sub>	1.8 $\pm$ 0.6	4.5 $\pm$ 0.2	2.0 $\pm$ 0.4	2.2 $\pm$ 0.8	4.2 $\pm$ 0.5	10.1 $\pm$ 0.2	0.7 $\pm$ 0.4	0.7 $\pm$ 1.0	-

Furthermore, POX reactivation was tested. Not surprisingly, the commercial compounds **1–2** and **5** were found not to be effective in this case [26]. The other commercial compounds **3–4** presented increased reactivation of POX-inhibited *HssAChE* at both determined concentrations (around 22% at 10  $\mu\text{M}$ ). The previously known compounds **6–9** showed lower reactivation ability up to 14% at human attainable concentration. The newly prepared compounds were found to be poor or average reactivators of POX-inhibited *HssAChE*, with the exception of compounds **15** (59%) and **22** (43%) at 10  $\mu\text{M}$ . These two compounds exceeded all commercially and previously known reactivators tested in this study against POX-induced inhibition.

The MePOX reactivation showed some similarities with POX reactivation. The commercial compounds **2** and **5** were found to be poor reactivators. However, surprisingly, the reactivation of compound **1** was found to be better at both concentrations (up to 30%) compared to POX reactivation (up to 11%). Nevertheless, commercial compounds **3–4** showed enhanced reactivation of MePOX-inhibited *HssAChE* at human attainable concentration (45 and 60% at 10  $\mu\text{M}$ ) [15]. The previously known compounds **6–9** also appeared to be promising MePOX reactivators, with a maximum of 41% at 10  $\mu\text{M}$  for compound **9**. The newly prepared oximes showed decreased reactivation of MePOX-inhibited *HssAChE* compared to the standards, with two compounds, **13** (17%) and **23** (21%), displayed some effect at 10  $\mu\text{M}$  concentration.

The poor reactivation of DFP-inhibited *HssAChE* was expected [15]. The previous experiments were confirmed by all standards **1–9**, where only compound **4** had some effective in vitro reactivation [27]. The newly prepared compounds also fulfilled these findings with minor or poor reactivation of DFP-inhibited *HssAChE*.

When the reactivation data at various concentrations were taken into account, some compounds (e.g., **15**, **16**, **22**) were shown to be better reactivators at lower concentration (10  $\mu\text{M}$ ), compared to their reactivation data at higher concentration (100  $\mu\text{M}$ ). These reactivation results can be explained by mixed reactivation-inhibition behavior of newly prepared compounds at various concentrations [28]. For this purpose, the inhibitory effect towards *HssAChE* of selected reactivators (**1–9**, **15–16** and **22–23**) was determined (Table 1). The commercial compounds **1–5** were shown to be poor *HssAChE* inhibitors, with the best inhibitory ability exhibited by trimedoxime (**4**; 167  $\mu\text{M}$ ). Two previously known reactivators, **7** (29  $\mu\text{M}$ ) and **8** (80  $\mu\text{M}$ ), showed even better *HssAChE* inhibition. Subsequently, compounds **4** and **7–8**, as the best *AChE* inhibitors among the standards, showed the above-mentioned mixed reactivation-inhibition effect for MePOX reactivation. Similarly, some newly prepared compounds (**15–16**, **22**) were found to be potent *HssAChE* inhibitors. In accordance with our hypothesis, compound **16** ( $\text{IC}_{50}$  6  $\mu\text{M}$ ) was shown to be a weaker reactivator of POX-inhibited *HssAChE* at a concentration of 100  $\mu\text{M}$  (7%) than at 10  $\mu\text{M}$  (9%), while it greatly inhibited *HssAChE* at the 100  $\mu\text{M}$  concentration (screening concentration 100  $\mu\text{M}$   $\gg$   $\text{IC}_{50}$  6  $\mu\text{M}$ ). At 10  $\mu\text{M}$ , compound **16** was found to be a slightly better reactivator (9%), while its inhibition ability decreased ten-fold, and it was closer to its  $\text{IC}_{50}$  value (6  $\mu\text{M}$ ). Similarly, compound **15** (screening concentration 100  $\mu\text{M}$   $\gg$   $\text{IC}_{50}$  24  $\mu\text{M}$ ) and compound **22** (screening concentration 100  $\mu\text{M}$   $\gg$   $\text{IC}_{50}$  45  $\mu\text{M}$ ) confirmed the mixed reactivation-inhibition hypothesis during POX reactivation, while compound **23** (screening concentration 100  $\mu\text{M}$   $\approx$   $\text{IC}_{50}$  90  $\mu\text{M}$ ) did not accurately fulfil this trend.

### 3.2. Molecular Modelling Results and SAR Discussion

The molecular modelling study was performed with oximes **3**, **9** and **23** to rationalize their interactions with GA-inhibited *HssAChE* [29]. Oxime **3** was chosen as a known commercial standard that is able to reactivate GA-inhibited *AChE* [30]. Additionally, oxime **9** was selected from among the previously prepared compounds as one of the best reactivators of GA-inhibited *HssAChE* [17]. Oxime **23** was selected as the best reactivator of GA-induced toxicity in vitro from among the newly prepared compounds.

The molecular modelling study was performed to better understand the in vitro results. The crystal structure of *HssAChE* in complex with fasciculin 2 (pdb 1b41) was chosen as a crystal structure with good structural resolution (2.76 Å) [31]. The fasciculin molecule was deleted, while the molecule of GA was manually attached to the catalytic triad residue Ser203, and the whole molecule of GA-inhibited *HssAChE* was minimized using Autodock Tools (ADT) [32]. The important aromatic residues within the *HssAChE* active site were selected as flexible residues, including the GA-Ser203 moiety. The molecules of three reactivators were also minimized by ADT. The molecular modelling was performed by Autodock Vina [33].

Compound **3** (the lowest binding energy  $-5.7$  kcal/mol) displayed typical interactions with AChE aromatic residues (Figure 5). The oxime-pyridinium ring was attached to Trp86 (3.6 Å), while the distance between oximate oxygen and GA phosphorus atom (6.8 Å) was found to be longer than previously observed results. The second pyridinium ring was stabilized via interactions with aromatic residues of the peripheral aromatic site (PAS), namely Phe338 (3.4 Å), Trp286 (4.2 Å), Tyr124 (4.0 Å) and Tyr341 (3.5 Å). The oxygen atom in the connecting linker seemed to be stabilized by interactions with phenolic moieties of Tyr124 (2.6 Å), Tyr337 (3.8 Å) and Tyr 341 (3.7 Å). Compound **9** (the lowest binding energy  $-5.5$  kcal/mol) showed similar results to compound **3**, with some exceptions in terms of flexible residues (Figures 5 and 6). In this case, the oxime pyridinium ring was stacked to Trp86 (3.6 Å) and the distance between the oxime and the GA phosphorus atom (5.1 Å) was better than previously published results. Not surprisingly, the non-oxime pyridinium ring was stabilized in PAS by Phe338 (3.6 Å), Trp286 (3.6 Å), Tyr124 (4.3 Å) and Tyr341 (3.6 Å), where the flexible residue Tyr341 was highly distorted compared to the same residue in the case of compound **3**. The double bond in the linker seemed to be stabilized by  $\pi$ - $\pi$  interaction with Tyr337 (4.0 Å). The carbamoyl moiety displayed important hydrogen bonds with Trp286 (2.2 Å) and Phe295 (2.9 Å). Compound **23** (the lowest binding energy  $-6.4$  kcal/mol) presented different binding when the amidoxime pyridinium ring was attached to Trp86 (3.6 Å), and amidoxime moiety was not located far from GA phosphorus (5.3 Å; Figure 6). The second ring bearing oxime moiety was stabilized in PAS by Phe338 (3.5 Å), Trp286 (3.7 Å), Tyr124 (3.6 Å) and Tyr341 (3.6 Å). The amidoxime moiety was further hydrogen bonded with Gly120 (3.3 Å) and Glu202 (2.1 Å).

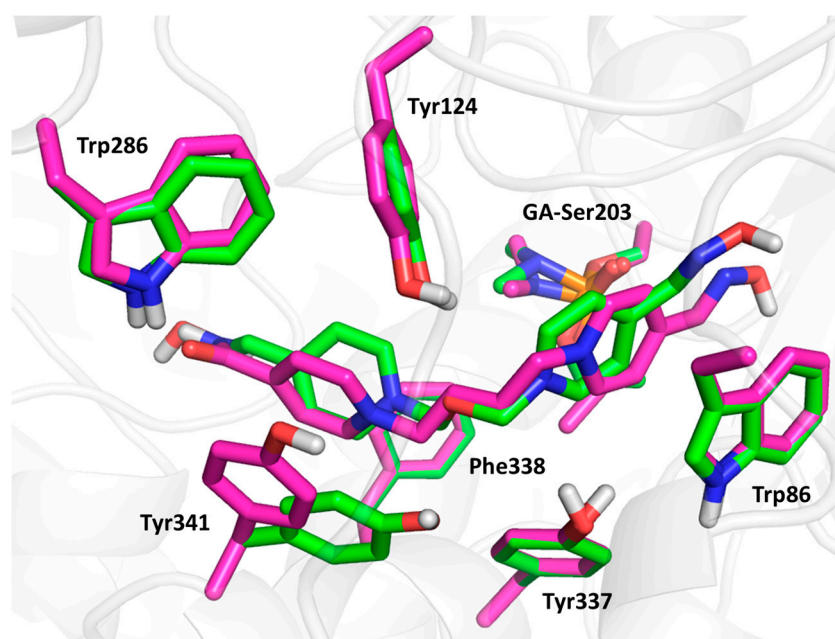


**Figure 5.** The molecular modelling results with selected flexible residues of compound **3** (in green) and compound **9** (in magenta).

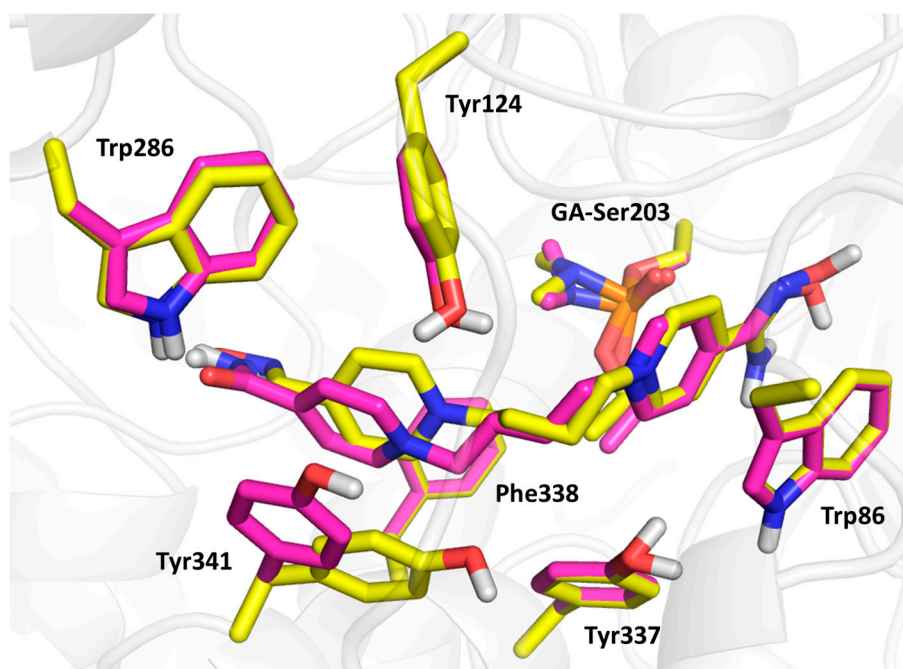


**Figure 6.** The molecular modelling results with selected flexible residues of compound **9** (in magenta) and compound **23** (in yellow).

Taken together, compound **9** showed more important interactions with GA-inhibited *HssAChE* active sites compared to compounds **3** and **23** [29]. This might be a reason for its increased reactivation ability in the case of GA-induced *in vitro* inhibition. The lower reactivation efficacy of compound **3** might be explained by its different interactions within the GA-*HssAChE* active site with inappropriate reactivator accommodation between Trp86 and PAS residues. Conversely, the lower *in vitro* reactivation efficacy of compound **23** might be related to the favorable structure with stabilized amidoxime moiety positioned close to GA-Ser203, while the spatial structure with oxime moiety positioned close to GA-Ser203 was found to be less favorable.

Concerning the SAR of oxime reactivators for GA or OP pesticide-inhibited *HssAChE*, several important attributes should be considered. Firstly, the bisquaternary mono-oximes were already found to be satisfactory reactivators of GA- or pesticide-inhibited AChE compared to bis-oximes [34]. The 4-positioned oxime moiety on the pyridinium scaffold has been used and proposed many times as being optimal for reactivation due to its pKa [35]. Furthermore, the connecting linkage between heteroarenium rings in the length of 3–4 C–C atoms was highlighted in the case of GA- or pesticide-inhibited AChE [36]. In this case, the newly prepared compounds with 4-membered linkers showed results equivalent to previously prepared series with 3-membered linkers with analogous non-oxime moieties. Additionally, the heteroarenium part of the molecule without oxime moiety was found to be very important for proper reactivation effects in the case of various OPs. The second heteroarenium ring was determined to be an important moiety for interactions with aromatic amino acid residues in the PAS region. Its modification by pyridinium, quinolinium or isoquinolinium moieties (**11–13**) did not lead to enhanced reactivation of GA or OP pesticide inhibited *HssAChE* [15]. However, its modification by various moieties bound in the 4-position of pyridinium scaffold showed better reactivation compared to known and analogous bis-oxime **7**. Namely, some newly prepared compounds with hydrophobic (**15**-tertbutyl) or hydrophilic moieties (**22**-carbonitrile and **23**-amidoxime) were found to be promising reactivators of selected OP pesticide inhibited *HssAChE*. Their increased reactivation ability might be explained by additional interactions with PAS amino acid residues, where tertbutyl (**15**) was proven to interact with aromatic residues, and carbonitrile (**22**) or amidoxime (**23**) are available for hydrogen bonding [37,38]. For the above-mentioned reasons,

the second heteroarenium part of the molecule is the essential molecular fragment, and should be properly designed for enhanced reactivation of OP inhibited *HssAChE* [34].

## 4. Experimental Section

### 4.1. Chemical Preparation

Solvents (acetone, DMF, MeCN) and reagents were purchased from Sigma-Aldrich (Prague, Czech Republic) and used without further purification. Reactions were monitored by TLC using DC-Alufolien Cellulose F (Merck, Darmstadt, Germany) and mobile phase BuOH-CH<sub>3</sub>COOH-H<sub>2</sub>O 5:1:2, detection by solution of Dragendorff reagent (solution containing 10 mL CH<sub>3</sub>COOH, 50 mL H<sub>2</sub>O and 5 mL of basic solution prepared by mixing of two fractions—fraction A: 850 mg Bi(NO<sub>3</sub>)<sub>3</sub>, 40 mL H<sub>2</sub>O, 10 mL CH<sub>3</sub>COOH; fraction B: 8 g KI, 20 mL H<sub>2</sub>O). Melting points were measured on micro heating stage PHMK 05 (VEB Kombinat Nagema, Radebeul, Germany) and were uncorrected.

NMR spectra were generally recorded at Varian Gemini 300 (<sup>1</sup>H 300 MHz, <sup>13</sup>C 75 MHz, Varian, Palo Alto, CA, USA). In all cases, the chemical shift values for <sup>1</sup>H spectra are reported in ppm (δ) relative to residual DMSO (δ 2.50) or D<sub>2</sub>O (δ 4.79), shift values for <sup>13</sup>C spectra are reported in ppm (δ) relative to solvent peak dimethylsulfoxide—*d*<sub>6</sub> δ 39.43. Signals are quoted as s (singlet), d (doublet), t (triplet) and m (multiplet).

The mass spectra (MS respectively MSn) were measured on a LCQ FLEET ion trap and evaluated using Xcalibur v 2.5.0 software (both Thermo Fisher Scientific, San Jose, CA, USA). The sample was dissolved in deionized water (Goro, s.r.o., Prague, Czech Republic), and injected continuously (8 μL/min) by Hamilton syringe into electrospray ion source. The parameters of electrospray were set up as follows: sheath gas flow rate 20 arbitrary units, aux gas flow rate 5 arbitrary units, sweep gas flow rate 0 arbitrary units, spray voltage 5 kV, capillary temperature 275 °C, capillary voltage 13 V, tube lens 100 V.

### 4.2. Preparation of Bisquaternary Salts

Initially the monoquaternary semi-product was prepared: a solution of the 4-hydroxyiminomethylpyridine (4.0 g, 32.8 mM) and 1,4-dibromobutane (19.6 mL, 163.8 mM) in acetone (30 mL) was stirred at reflux for 8 h [15]. The reaction mixture was cooled to room temperature and the crystalline crude product collected by filtration and washed with acetone (3 × 20 mL). The solid crude product was crystallized from MeCN (1 g of crude product per 100 mL of MeCN), where the boiling mixture was filtered under a reduced pressure. The filtrate was evaporated under a reduced pressure to produce the pure monoquaternary salt of 1-(4-bromobutyl)-4-hydroxyiminomethylpyridinium bromide (75%).

Secondly, the synthesis of the bisquaternary salt was completed. A solution of the monoquaternary salt (0.50 g, 1.5 mM) and selected heteroaromatic compound (3.0 mM) in DMF or MeCN (10 mL) was stirred at 70–80 °C for 8 h. The reaction mixture was cooled to room temperature and portioned with acetone (80 mL); the crystalline crude product was collected by filtration, washed with acetone (3 × 20 mL) and crystallized from boiling MeCN. The pure bisquaternary salt was obtained as the solid compound insoluble in boiling MeCN as the mixtures of cis/trans oxime isomers.

### 4.3. Prepared Monoquaternary Salt

1-(4-Bromobutyl)-4-((hydroxyimino)methyl)pyridinium bromide. M.p. 154–155 °C. Yield 91%. <sup>1</sup>H-NMR (300 MHz, DMSO *d*<sub>6</sub>): δ (ppm) 12.82 (s, 1H, NOH), 9.08 (d, 2H, *J* = 6.5 Hz, H-2,6), 8.44 (s, 1H, -CH=NOH), 8.25 (d, 2H, *J* = 6.4 Hz, H-3,5), 4.64 (t, 2H, *J* = 7.2 Hz, N-CH<sub>2</sub>-), 3.57 (t, 2H, *J* = 6.6 Hz, CH<sub>2</sub>-Br), 2.08–2.01 (m, 2H, -CH<sub>2</sub>-), 1.86–1.80 (m, 2H, -CH<sub>2</sub>-). <sup>13</sup>C-NMR (75 MHz, DMSO *d*<sub>6</sub>): δ (ppm) 148.32, 145.01, 144.88, 124.04, 59.25, 33.91, 29.29, 28.56. EA: calculated 35.53% C, 4.17% H, 8.29% N; found 35.58% C, 4.12% H, 8.25% N. ESI-MS: *m/z* 257.0 [M]<sup>+</sup> (calculated [C<sub>10</sub>H<sub>14</sub>BrN<sub>2</sub>O]<sup>+</sup> 257.03).

#### 4.4. Prepared Bisquaternary Salts

*4-Hydroxyiminomethyl-1,1'-(but-1,4-diyl)-bispyridinium dibromide (10)* [39]. M.p. 243–244 °C. Yield 48%. <sup>1</sup>H-NMR (300 MHz, DMSO *d*<sub>6</sub>): δ (ppm) 12.84 (s, 1H, NOH), 9.18 (d, 2H, *J* = 6.2 Hz, H-2,6), 9.12 (d, 2H, *J* = 6.2 Hz, H-2',6'), 8.67–8.59 (m, 1H, H-4'), 8.46 (s, 1H, -CH=NOH), 8.25 (d, 2H, *J* = 6.2 Hz, H-3,5), 8.22–8.15 (m, 2H, H-3',5'), 4.80–4.62 (m, 4H, N-CH<sub>2</sub>-), 1.97 (m, 4H, N-CH<sub>2</sub>-CH<sub>2</sub>-). <sup>13</sup>C-NMR (75 MHz, DMSO *d*<sub>6</sub>): δ (ppm) 148.30, 145.53, 145.01, 144.98, 144.75, 128.05, 124.00, 59.63, 59.19, 27.06, 26.95. EA: calculated 43.19% C, 4.59% H, 10.07% N; found 43.29% C, 4.75% H, 10.08% N. ESI-MS: *m/z* 128.6 [M/2]<sup>2+</sup> (calculated [C<sub>15</sub>H<sub>19</sub>N<sub>3</sub>O/2]<sup>2+</sup> 128.58).

*4-Hydroxyiminomethyl-1,1'-(but-1,4-diyl)-1-pyridinium-1'-pyridazinium dibromide (11)*. M.p. 222–224 °C. Yield 71%. <sup>1</sup>H-NMR (300 MHz, DMSO *d*<sub>6</sub>): δ (ppm) 10.05 (d, 1H, *J* = 5.8 Hz, H-6'), 9.65 (d, 1H, *J* = 4.8 Hz, H-3'), 9.11 (d, 2H, *J* = 6.0 Hz, H-2,6), 8.80–8.73 (m, 1H, H-4'), 8.67–8.60 (m, 1H, H-5'), 8.45 (s, 1H, -CH=NOH), 8.26 (d, 2H, *J* = 6.0 Hz, H-3,5), 4.91 (t, 2H, *J* = 6.3 Hz, N'-CH<sub>2</sub>-), 4.68 (t, 2H, *J* = 6.3 Hz, N-CH<sub>2</sub>-), 2.10–1.96 (m, 4H, N-CH<sub>2</sub>-CH<sub>2</sub>-). <sup>13</sup>C-NMR (75 MHz, DMSO *d*<sub>6</sub>): δ (ppm) 154.47, 150.12, 148.34, 145.03, 136.58, 136.01, 124.00, 63.44, 59.23, 26.98, 25.73. EA: calculated 40.21% C, 4.34% H, 13.40% N; found 40.09% C, 4.49% H, 13.27% N. ESI-MS: *m/z* 129.1 [M/2]<sup>2+</sup> (calculated [C<sub>14</sub>H<sub>18</sub>N<sub>4</sub>O/2]<sup>2+</sup> 129.08).

*4-Hydroxyiminomethyl-1,1'-(but-1,4-diyl)-1-pyridinium-1'-quinolinium dibromide (12)* [39]. M.p. 177–179 °C. Yield 21%. <sup>1</sup>H-NMR (300 MHz, DMSO *d*<sub>6</sub>): δ (ppm) 9.68 (d, 1H, *J* = 5.8 Hz, H-2'), 9.34 (d, 1H, *J* = 8.4 Hz, H-8'), 9.12 (d, 2H, *J* = 6.2 Hz, H-2,6), 8.71 (d, 1H, *J* = 8.8 Hz, H-4'), 8.53 (d, 1H, *J* = 8.1 Hz, H-5'), 8.45 (s, 1H, -CH=NOH), 8.33–8.17 (m, 4H, H-3,3',5,7'), 8.11–8.02 (m, 1H, H-6'), 5.17 (t, 2H, *J* = 7.0 Hz, N'-CH<sub>2</sub>-), 4.71 (t, 2H, *J* = 7.0 Hz, N-CH<sub>2</sub>-), 2.20–1.93 (m, 4H, N-CH<sub>2</sub>-CH<sub>2</sub>-). <sup>13</sup>C-NMR (75 MHz, DMSO *d*<sub>6</sub>): δ (ppm) 149.71, 148.29, 147.41, 145.01, 137.33, 135.58, 130.70, 129.81, 129.66, 123.99, 122.16, 119.00, 59.33, 58.35, 27.36, 25.88. EA: calculated 48.85% C, 4.53% H, 8.99% N; found 48.41% C, 4.63% H, 9.06% N. ESI-MS: *m/z* 153.6 [M/2]<sup>2+</sup> (calculated [C<sub>19</sub>H<sub>21</sub>N<sub>3</sub>O/2]<sup>2+</sup> 153.59).

*4-Hydroxyiminomethyl-1,1'-(but-1,4-diyl)-1-pyridinium-1'-isoquinolinium dibromide (13)* [39]. M.p. 205–206 °C. Yield 26%. <sup>1</sup>H-NMR (300 MHz, DMSO *d*<sub>6</sub>): δ (ppm) 10.26 (s, 1H, H-1'), 9.12 (d, 2H, *J* = 6.2 Hz, H-2,6), 8.87 (d, 1H, *J* = 6.7 Hz, H-3'), 8.64 (d, 1H, *J* = 6.7 Hz, H-4'), 8.51 (d, 1H, *J* = 8.2 Hz, H-8'), 8.44 (s, 1H, -CH=NOH), 8.38 (d, 1H, *J* = 8.2 Hz, H-5'), 8.32–8.21 (m, 3H, H-3,5,7'), 8.12–8.04 (m, 1H, 6'), 4.83 (t, 2H, *J* = 6.7 Hz, N-CH<sub>2</sub>-), 4.70 (t, 2H, *J* = 6.7 Hz, N'-CH<sub>2</sub>-), 2.18–1.94 (m, 4H, N-CH<sub>2</sub>-CH<sub>2</sub>-). <sup>13</sup>C-NMR (75 MHz, DMSO *d*<sub>6</sub>): δ (ppm) 150.08, 148.30, 145.02, 136.92, 136.82, 134.85, 131.09, 130.33, 127.19, 127.13, 125.80, 124.99, 59.67, 59.29, 27.03, 26.81. EA: calculated 48.85% C, 4.53% H, 8.99% N; found 48.53% C, 4.75% H, 8.78% N. ESI-MS: *m/z* 153.6 [M]<sup>2+</sup> (calculated [C<sub>19</sub>H<sub>19</sub>N<sub>3</sub>O]<sup>2+</sup> 153.59).

*4-Hydroxyiminomethyl-4'-methyl-1,1'-(but-1,4-diyl)-bispyridinium dibromide (14)*. M.p. 190–192 °C. Yield 47%. <sup>1</sup>H-NMR (300 MHz, D<sub>2</sub>O): δ (ppm) 8.83 (d, 2H, *J* = 6.2 Hz, H-2,6), 8.65 (d, 2H, *J* = 6.0 Hz, H-2',6'), 8.39 (s, 1H, -CH=NOH), 8.21 (d, 2H, *J* = 6.0 Hz, H-3,5), 7.89 (d, 2H, *J* = 6.0 Hz, H-3',5'), 4.70–4.58 (m, 4H, N-CH<sub>2</sub>-,N'-CH<sub>2</sub>-), 2.23 (s, 3H, -CH<sub>3</sub>), 2.15–2.08 (m, 4H, N-CH<sub>2</sub>-CH<sub>2</sub>-). <sup>13</sup>C-NMR (75 MHz, D<sub>2</sub>O *d*<sub>6</sub>): δ (ppm) 161.06, 149.47, 146.87, 145.09, 143.67, 129.43, 125.60, 61.09, 60.50, 30.89. EA: calculated 44.57% C, 4.91% H, 9.75% N, found 44.13% C, 5.00% H, 9.61% N. ESI-MS: *m/z* 270.0 [M<sup>2+</sup> - H] (calculated for [C<sub>16</sub>H<sub>21</sub>N<sub>3</sub>O<sup>2+</sup> - H] 270.17).

*4-Hydroxyiminomethyl-4'-(1,1-dimethylethyl)-1,1'-(but-1,4-diyl)-bispyridinium dibromide (15)*. M.p. 146–148 °C. Yield 75%. <sup>1</sup>H-NMR (300 MHz, D<sub>2</sub>O): δ (ppm) 8.83 (d, 2H, *J* = 6.2 Hz, H-2,6), 8.70 (d, 2H, *J* = 6.2 Hz, H-2',6'), 8.38 (s, 1H, -CH=NOH), 8.21 (d, 2H, *J* = 6.2 Hz, H-3,5), 8.08 (d, 2H, *J* = 6.2 Hz, H-3',5'), 4.68–4.59 (m, 4H, N-CH<sub>2</sub>-,N'-CH<sub>2</sub>-), 2.14–2.08 (m, 4H, N-CH<sub>2</sub>-CH<sub>2</sub>-), 1.40 (s, 9H, -CH<sub>3</sub>). <sup>13</sup>C-NMR (75 MHz, D<sub>2</sub>O *d*<sub>6</sub>): δ (ppm) 159.71, 158.49, 157.67, 155.86, 154.35, 134.61, 134.25, 70.23, 70.06, 39.88, 36.84. EA: calculated 48.22% C, 5.75% H, 8.88% N, found 47.91% C, 6.13% H, 8.54% N. ESI-MS: *m/z* 156.5 [M<sup>2+</sup> / 2] (calculated for [C<sub>19</sub>H<sub>27</sub>N<sub>3</sub>O<sup>2+</sup> / 2] 156.61).

**4-Hydroxyiminomethyl-4'-phenyl-1,1'-(but-1,4-diyl)-bispyridinium dibromide (16).** M.p. 236–238 °C. Yield 45%. <sup>1</sup>H-NMR (300 MHz, DMSO *d*<sub>6</sub>): δ (ppm) 9.19 (d, 2H, *J* = 6.2 Hz, H-2,6), 9.12 (d, 2H, *J* = 6.2 Hz, H-2',6'), 8.56 (d, 2H, *J* = 6.2 Hz, H-3,5), 8.46 (s, 1H, -CH=NOH), 8.26 (d, 2H, *J* = 6.2 Hz, H-3',5'), 8.14–8.07 (m, 2H, Ph), 7.69–7.62 (m, 3H, Ph), 4.79–4.61 (m, 4H, N-CH<sub>2</sub>-, N'-CH<sub>2</sub>-), 2.10–1.94 (m, 4H, N-CH<sub>2</sub>-CH<sub>2</sub>-). <sup>13</sup>C-NMR (75 MHz, DMSO *d*<sub>6</sub>): δ (ppm) 154.61, 148.32, 145.03, 144.79, 133.43, 132.09, 129.63, 128.07, 124.45, 124.02, 59.27, 58.81, 27.01, 26.98. EA: calculated 51.14% C, 4.70% H, 8.52% N; found 50.92% C, 4.96% H, 8.08% N. ESI-MS: *m/z* 166.6 [M/2]<sup>2+</sup> (calculated [C<sub>21</sub>H<sub>23</sub>N<sub>3</sub>O/2]<sup>2+</sup> 166.59).

**4-Hydroxyiminomethyl-4'-phenylmethyl-1,1'-(but-1,4-diyl)-bispyridinium dibromide (17).** M.p. not measured (amorphous). Yield 11%. <sup>1</sup>H-NMR (300 MHz, DMSO *d*<sub>6</sub>): δ (ppm) 9.37 (d, 2H, *J* = 6.0 Hz, H-2,6), 9.14 (d, 2H, *J* = 6.0 Hz, H-2',6'), 8.46 (s, 1H, -CH=NOH), 8.39 (d, 2H, *J* = 6.0 Hz, H-3,5), 8.27 (d, 2H, *J* = 6.0 Hz, H-3',5'), 7.90–7.77 (m, 3H, Ph), 7.68–7.60 (m, 2H, Ph), 4.86–4.77 (m, 2H, N-CH<sub>2</sub>-), 4.75–4.66 (m, 2H, N'-CH<sub>2</sub>-), 2.10–2.00 (m, 6H, Ph-CH<sub>2</sub>-, N-CH<sub>2</sub>-CH<sub>2</sub>-). <sup>13</sup>C-NMR (75 MHz, DMSO *d*<sub>6</sub>): δ (ppm) 151.63, 148.34, 145.74, 145.09, 145.03, 134.82, 134.05, 130.29, 129.12, 129.04, 126.83, 124.02, 59.91, 59.24, 27.05, 26.96. EA: calculated 52.09% C, 4.97% H, 8.28% N; found 52.33% C, 4.79% H, 8.64% N. ESI-MS: *m/z* 346.0 [M<sup>2+</sup> – H] (calculated [C<sub>22</sub>H<sub>25</sub>N<sub>3</sub>O<sup>2+</sup> – H] 346.20).

**4-Hydroxyiminomethyl-4'-hydroxymethyl-1,1'-(but-1,4-diyl)-bispyridinium dibromide (18).** M.p. 162–164 °C. Yield 45%. <sup>1</sup>H-NMR (300 MHz, DMSO *d*<sub>6</sub>): δ (ppm) 9.22–9.01 (m, 4H, H-2,2',6,6'), 8.45 (s, 1H, -CH=NOH), 8.25 (d, 2H, *J* = 6.0 Hz, H-3',5'), 8.05 (d, 2H, *J* = 5.9 Hz, H-3,5), 4.81 (s, 2H, -CH<sub>2</sub>-OH), 4.76–4.60 (m, 4H, N-CH<sub>2</sub>-, N'-CH<sub>2</sub>-), 2.05–1.89 (m, 2H, N-CH<sub>2</sub>-CH<sub>2</sub>-). <sup>13</sup>C-NMR (75 MHz, DMSO *d*<sub>6</sub>): δ (ppm) 148.31, 145.03, 144.98, 144.04, 124.29, 124.01, 61.07, 59.24, 59.01, 26.99. EA: calculated 42.98% C, 4.73% H, 9.40% N, found 42.63% C, 4.98% H, 9.04% N. ESI-MS: *m/z* 286.0 [M<sup>2+</sup> – H] (calculated for [C<sub>16</sub>H<sub>21</sub>N<sub>3</sub>O<sub>2</sub><sup>2+</sup> – H] 286.16).

**4-Hydroxyiminomethyl-4'-methylcarbonyl-1,1'-(but-1,4-diyl)-bispyridinium dibromide (19).** M.p. 217–219 °C. Yield 18%. <sup>1</sup>H-NMR (300 MHz, D<sub>2</sub>O): δ (ppm) 9.11 (d, 2H, *J* = 6.0 Hz, H-2',6'), 8.84 (d, 2H, *J* = 6.0 Hz, H-2,6), 8.49 (d, 2H, *J* = 6.2 Hz, H-3',5'), 8.38 (s, 1H, -CH=NOH), 8.21 (d, 2H, *J* = 6.0 Hz, H-3,5), 4.69–4.64 (m, 4H, N-CH<sub>2</sub>-, N'-CH<sub>2</sub>-), 2.80 (s, 3H, -CH<sub>3</sub>), 2.20–2.15 (m, 4H, N-CH<sub>2</sub>-CH<sub>2</sub>-). <sup>13</sup>C-NMR (75 MHz, D<sub>2</sub>O *d*<sub>6</sub>): δ (ppm) 198.29, 149.54, 149.40, 146.79, 146.51, 146.48, 145.04, 127.10, 125.53, 61.72, 60.93, 30.80, 27.87, 27.24. EA: calculated 44.47% C, 4.61% H, 9.15% N, found 44.08% C, 4.77% H, 9.15% N. ESI-MS: *m/z* 149.5 [M<sup>2+</sup> / 2] (calculated for [C<sub>17</sub>H<sub>21</sub>N<sub>3</sub>O<sub>2</sub><sup>2+</sup> / 2] 149.58).

**4-Carboxy-4'-hydroxyiminomethyl-1,1'-(but-1,4-diyl)-bispyridinium dibromide (20).** M.p. decomp. 230 °C. Yield 51%. <sup>1</sup>H-NMR (300 MHz, DMSO *d*<sub>6</sub>): δ (ppm) 9.33 (d, 2H, *J* = 6.2 Hz, H-2,6), 9.12 (d, 2H, *J* = 6.2 Hz, H-2',6'), 8.48 (d, 2H, *J* = 6.0 Hz, H-3,5), 8.45 (s, 1H, -CH=NOH), 8.25 (d, 2H, *J* = 6.0 Hz, H-3',5'), 4.88–4.62 (m, 4H, N-CH<sub>2</sub>-, N'-CH<sub>2</sub>-), 2.06–1.90 (m, 4H, N-CH<sub>2</sub>-CH<sub>2</sub>-). <sup>13</sup>C-NMR (75 MHz, DMSO *d*<sub>6</sub>): δ (ppm) 163.53, 148.33, 146.15, 145.37, 145.02, 127.28, 124.00, 60.00, 59.19, 27.08, 26.89. EA: calculated 41.67% C, 4.15% H, 9.11% N; found 41.34% C, 4.40% H, 9.24% N. ESI-MS: *m/z* 150.6 [M/2]<sup>2+</sup> (calculated [C<sub>16</sub>H<sub>19</sub>N<sub>3</sub>O<sub>3</sub>/2]<sup>2+</sup> 150.57).

**4-Ethylcarboxy-4'-hydroxyiminomethyl-1,1'-(but-1,4-diyl)-bispyridinium dibromide (21).** M.p. 174–176 °C. Yield 8%. <sup>1</sup>H-NMR (300 MHz, DMSO *d*<sub>6</sub>): δ (ppm) 9.36 (d, 2H, *J* = 6.0 Hz, H-2,6), 9.11 (d, 2H, *J* = 6.0 Hz, H-2',6'), 8.53 (d, 2H, *J* = 6.0 Hz, H-3,5), 8.45 (s, 1H, -CH=NOH), 8.25 (d, 2H, *J* = 6.0 Hz, H-3',5'), 4.85–4.76 (m, 2H, N-CH<sub>2</sub>-), 4.72–4.63 (m, 2H, N'-CH<sub>2</sub>-), 4.44 (q, 2H, *J*<sub>12</sub> = *J*<sub>22</sub> = 7.0 Hz, COO-CH<sub>2</sub>-), 2.05–1.92 (m, 4H, N-CH<sub>2</sub>-CH<sub>2</sub>-), 1.37 (t, 3H, *J* = 7.0 Hz, -CH<sub>3</sub>). <sup>13</sup>C-NMR (75 MHz, DMSO *d*<sub>6</sub>): δ (ppm) 162.00, 148.31, 146.28, 144.99, 144.96, 143.80, 127.16, 123.98, 62.89, 60.11, 59.16, 27.06, 26.85, 13.81. EA: calculated 44.19% C, 4.74% H, 8.59% N, found 43.84% C, 5.19% H, 8.10% N. ESI-MS: *m/z* 164.5 [M<sup>2+</sup> / 2] (calculated for [C<sub>18</sub>H<sub>23</sub>N<sub>3</sub>O<sub>3</sub><sup>2+</sup> / 2] 164.59).

**4-Carbonitril-4'-hydroxyiminomethyl-1,1'-(but-1,4-diyl)-bispyridinium dibromide (22).** M.p. 247–249 °C. Yield 21%. <sup>1</sup>H-NMR (300 MHz, DMSO *d*<sub>6</sub>): δ (ppm) 9.50 (d, 2H, *J* = 6.2 Hz, H-2,6), 9.12 (d, 2H, *J* = 6.2 Hz, H-2',6'), 8.76 (d, 2H, *J* = 6.2 Hz, H-3,5), 8.45 (s, 1H, -CH=NOH), 8.25 (d, 2H, *J* = 6.0 Hz, H-3',5'), 4.89–4.59 (m, 4H, N-CH<sub>2</sub>-, N'-CH<sub>2</sub>-), 2.10–1.88 (m, 4H, N-CH<sub>2</sub>-CH<sub>2</sub>-). <sup>13</sup>C-NMR (75 MHz,

DMSO  $d_6$ ):  $\delta$  (ppm) 148.32, 146.23, 145.00, 130.96, 126.79, 124.06, 114.76, 60.60, 59.11, 26.90, 26.78. EA: calculated 43.46% C, 4.10% H, 12.67% N; found 43.16% C, 4.26% H, 12.51% N. ESI-MS:  $m/z$  141.1 [ $M^{2+}/2$ ] (calculated [ $C_{16}H_{18}N_4O^{2+}/2$ ] 141.08).

4-(1-Amino-1-hydroxyiminomethyl)-4'-hydroxyiminomethyl-1,1'-(but-1,4-diyl)-bispyridinium dibromide (**23**). M.p. 258 °C. Yield 51%.  $^1H$ -NMR (300 MHz, DMSO  $d_6$ ):  $\delta$  (ppm) 9.15–9.07 (m, 4H, H-2, 2', 6, 6'), 8.45 (s, 1H, -CH=NOH), 8.33 (d, 2H,  $J = 6.2$  Hz, H-3,5), 8.25 (d, 2H,  $J = 6.0$  Hz, H-3',5'), 6.46 (s, 2H, -NH<sub>2</sub>), 4.72–4.61 (m, 4H, N-CH<sub>2</sub>-, N'-CH<sub>2</sub>-), 2.02–1.91 (m, 4H, N-CH<sub>2</sub>-CH<sub>2</sub>-).  $^{13}C$ -NMR (75 MHz, DMSO  $d_6$ ):  $\delta$  (ppm) 148.31, 147.77, 146.92, 145.03, 144.99, 144.55, 124.01, 122.71, 59.23, 59.09, 26.94, 26.88. EA: calculated 40.44% C, 4.45% H, 14.74% N; found 40.16% C, 4.56% H, 14.35% N. ESI-MS:  $m/z$  157.6 [ $M^{2+}/2$ ] (calculated [ $C_{16}H_{21}N_5O_2^{2+}/2$ ] 157.59).

3,4-Dicarbamoyl-4'-hydroxyiminomethyl-1,1'-(but-1,4-diyl)-bispyridinium dibromide (**24**). M.p. decomposition at 191–193 °C. Yield 59%.  $^1H$ -NMR (300 MHz, DMSO  $d_6$ ):  $\delta$  (ppm) 9.50–9.26 (m, 2H, H-2',6'), 9.13 (d, 2H,  $J = 6.2$  Hz, H-2,6), 8.51–8.33 (m, 3H, -CH=NOH, H-3,5), 8.31–8.03 (m, 5H, -CONH<sub>2</sub>, H-5'), 4.86–4.61 (m, 4H, N-CH<sub>2</sub>-, N'-CH<sub>2</sub>-), 2.16–1.88 (m, 4H, N-CH<sub>2</sub>-CH<sub>2</sub>-).  $^{13}C$ -NMR (75 MHz, DMSO  $d_6$ ):  $\delta$  (ppm) 165.71, 164.01, 150.72, 148.60, 146.41, 145.43, 144.67, 134.39, 126.33, 124.30, 60.17, 59.48, 27.22, 27.09. EA: calculated 40.58% C, 4.21% H, 13.92% N; found 40.34% C, 4.35% H, 13.46% N. ESI-MS:  $m/z$  171.6 [ $M^{2+}/2$ ] (calculated [ $C_{17}H_{21}N_5O_3^{2+}/2$ ] 171.58).

#### 4.5. In Vitro Reactivation Assay

The reactivation ability was measured on a multichannel spectrophotometer Sunrise (Tecan, Salzburg, Austria). The previously used Ellman's procedure was slightly adapted [22]. Standard polystyrene microplates with 96 wells (Nunc, Roskilde, Denmark) were chosen as reaction cuvettes. Recombinant HssAChE (Sigma-Aldrich) was used throughout experiments. Tabun (GA; *O*-ethyl-*N,N*-dimethylphosphoramidocyanidate) was obtained from the Military Facility in Brno. Pesticides paraoxon (POX), methylparaoxon (MePOX) and diisopropylfluorophosphate (DFP) were purchased from Sigma-Aldrich (Prague, Czech Republic). 50 mM phosphate buffer pH 7.4 was used throughout all experiments.

The activity of the enzyme was adjusted to 0.002 U/ $\mu$ L. The inhibited enzyme was prepared directly before the testing of the potential reactivator. Phosphate buffer containing 1 mg/mL albumin, and a solution of enzyme (15  $\mu$ L) was incubated with 1  $\mu$ M GA or 10  $\mu$ M POX or 10  $\mu$ M MePOX or 100  $\mu$ M DFP (5  $\mu$ L) at room temperature to achieve 95% inhibition. The time of inhibition was selected with respect to the inhibition half-life of each inhibitor (GA—40 min, POX and MePOX—1 h, DFP—1 h 20 min).

One well was filled by the following chemicals: inhibited enzyme solution (20  $\mu$ L), phosphate buffer (60  $\mu$ L), 0.4 mg/mL 5,5'-dithio-bis-(2-nitrobenzoic)-acid (DTBN; 20  $\mu$ L). Cholinesterase was reactivated by the addition of 100  $\mu$ M or 10  $\mu$ M oxime-reactivator dissolved in the phosphate buffer. Enzyme activity was measured after 15 min incubation via addition of 1 mM acetylthiocholine chloride (20  $\mu$ L, ATChCl). Oximolysis was determined similarly by displacing enzyme with the phosphate buffer containing 1 mg/mL albumine. The microplate was gently shaken by the incorporated robotic system just before measurement. Absorbance was measured against phosphate buffer at 412 nm.

The reactivation ability was calculated according to the following equation.

$$(\%) = \frac{A_r - A_{ox}}{A_0 - A_i} \times 100 \quad (1)$$

$A_r$  indicates absorbance at 412 nm provided by cholinesterase reactivated by reactivator;  $A_{ox}$ —absorbance provided by oximolysis;  $A_0$ —absorbance provided by intact cholinesterase;  $A_i$ —absorbance provided by inhibited cholinesterase.

All measurements were performed in triplicate and the reactivation data are expressed as average value  $\pm$  standard deviation (SD).

#### 4.6. In Vitro Inhibition Assay

The multichannel spectrophotometer Sunrise (Tecan, Salzburg, Austria) was used for all measurements of *HssAChE* activity. The previously optimized Ellman's procedure was slightly adapted in order to estimate inhibitory properties *HssAChE* reactivators [15]. 96-well photometric microplates made from polystyrene (Nunc, Roskilde, Denmark) were used for measuring purposes. Recombinant *HssAChE* (Aldrich; commercially purified by affinity chromatography) was suspended in phosphate buffer (pH 7.4) to a final activity of 0.002 U/ $\mu$ L. Cholinesterase (5  $\mu$ L), a freshly mixed solution of 0.4 mg/mL 5,5'-dithio-bis(2-nitrobenzoic) acid (40  $\mu$ L), 1 mM acetylthiocholine chloride in phosphate buffer (20  $\mu$ L) and the appropriate concentration of inhibitor (1 mM–0.1 nM; 5  $\mu$ L) were injected per well. Absorbance was measured at 412 nm after 5 min incubation by automatic shaking of the microplate.

Percentage of inhibition (I) was calculated from the measured data as follows:

$$I = 1 - \frac{\Delta A_i}{\Delta A_0} \quad (2)$$

$\Delta A_i$  indicates absorbance change provided by cholinesterase exposed to anticholinergic compound.  $\Delta A_0$  indicates absorbance change caused by intact cholinesterase, where phosphate buffer was applied in the same way as the anticholinergic compound.

IC<sub>50</sub> was determined using Origin 6.1 (OriginLab Corporation, Northampton, MA, USA). Percentage of inhibition was calculated by Hill plot ( $n = 1$ ). The other plot variants (between  $-2$  and  $+2$ ) were not optimal and the coefficient of determination was lower compared to chosen method. Subsequently, IC<sub>50</sub> was computed.

#### 4.7. Molecular Docking Study

The structure of *HssAChE* was prepared from the crystal structure (pdb code b1b41) using Autodock Tools 1.5.6 (ADT) [31,32]. The fasciculine molecule was deleted and the molecule of tabun was manually added. The GA-inhibited *HssAChE* was minimized and prepared for calculation using ADT. The 3D affinity grid box was designed to include the full active and peripheral site of *HssAChE*. The number of grid points on the  $x$ -,  $y$ - and  $z$ -axes was 55, 55 and 55, with grid points separated by 0.400 Å. The important *HssAChE* aromatic residues (His447, Phe295, Phe297, Phe338, Trp86, Trp236, Trp286, Tyr72, Tyr124, Tyr337 and Tyr341) and GA-inhibited Ser203 were set up as flexible residues. The molecular model of ligand was built using ChemDraw 11.1, minimized with UCSF Chimera 1.3 (Amber Force field) in charged form and prepared by ADT [40]. The calculation was done using AutoDock Vina 1.1.2 [33]. The pdb files were obtained with iBabel 2.6. The visualization of enzyme-ligand interactions (Figures 5 and 6) was prepared using Pymol 1.1 [41].

## 5. Conclusions

A new series of mono-oxime *HssAChE* reactivators with tetramethylene linkage was designed as analogues of previously prepared compounds K048 (6) and K074 (7). Fifteen newly prepared compounds were synthesized and determined on the in vitro model of GA, POX, MePOX and DFP-inhibited *HssAChE*. The reactivation ability of the novel compounds was compared to the commercial standards and selected promising previously known compounds. Some novel compounds presented enhanced ability to reactivate OP-inhibited *HssAChE*, while at least two of them (15, 22) were able to exceed the reactivation potency of the already known compounds for POX-inhibited *HssAChE*. One compound (23) presented promising reactivation of GA-inhibited *HssAChE*. This reactivator was selected for a further molecular modelling experiment that confirmed the proposed and important interactions with PAS of *HssAChE*.

**Author Contributions:** Conceptualization, K.M. and K.K.; Synthesis D.M. and E.N.; Methodology, D.M. and D.J.; Validation, K.K., K.M. and D.J.; Writing-Original Draft Preparation, K.M. and K.K.; Funding Acquisition, K.M. and K.K.

**Funding:** The work was supported by Czech Science Foundation (no. 18-01734S), University of Hradec Kralove (VT2201-2018) and University of Defence (long-term organization development plan).

**Conflicts of Interest:** The authors declare no conflict of interest. The founding sponsors had no role in the design of the study; in the collection, analyses, or interpretation of data; in the writing of the manuscript, and in the decision to publish the results.

## References

1. Marrs, T.C. Organophosphate poisoning. *Pharmacol. Ther.* **1993**, *58*, 51–66. [[CrossRef](#)]
2. Bajgar, J. Organophosphates/nerve agent poisoning: Mechanism of action, diagnosis, prophylaxis, and treatment. *Adv. Clin. Chem.* **2004**, *38*, 151–193. [[PubMed](#)]
3. Saxena, A.; Sun, W.; Luo, C.; Myers, T.M.; Koplovitz, I.; Lenz, D.E.; Doctor, B.P. Bioscavenger for protection from toxicity of organophosphorus compounds. *J. Mol. Neurosci.* **2006**, *30*, 145–147. [[CrossRef](#)]
4. Newmark, J. Therapy for Nerve Agent Poisoning. *Arch. Neurol.* **2004**, *61*, 649–652. [[CrossRef](#)] [[PubMed](#)]
5. Bajgar, J.; Fusek, J.; Kassa, J.; Kuca, K.; Jun, D. Chemical Aspects of Pharmacological Prophylaxis against Nerve Agent Poisoning. *Curr. Med. Chem.* **2009**, *16*, 2977–2986. [[CrossRef](#)] [[PubMed](#)]
6. Doctor, B.P.; Raveh, L.; Wolfe, A.D.; Maxwell, D.M.; Ashani, Y. Enzymes as pretreatment drugs for organophosphate toxicity. *Neurosci. Biobehav. Rev.* **1991**, *15*, 123–128. [[CrossRef](#)]
7. Jokanovic, M.; Stojiljkovic, M.P. Current understanding of the application of pyridinium oximes as cholinesterase reactivators in treatment of organophosphate poisoning. *Eur. J. Pharmacol.* **2006**, *553*, 10–17. [[CrossRef](#)] [[PubMed](#)]
8. Bajgar, J.; Fusek, J.; Kuca, K.; Bartosova, L.; Jun, D. Treatment of Organophosphate Intoxication Using Cholinesterase Reactivators: Facts and Fiction. *Mini-Rev. Med. Chem.* **2007**, *7*, 461–466. [[CrossRef](#)] [[PubMed](#)]
9. Carletti, E.; Li, H.; Li, B.; Ekstrom, F.; Nicolet, Y.; Loiodice, M.; Gillon, E.; Froment, M.T.; Lockridge, O.; Schopfer, L.M.; et al. Aging of Cholinesterases Phosphorylated by Tabun Proceeds through O-Dealkylation. *J. Am. Chem. Soc.* **2008**, *130*, 16011–16020. [[CrossRef](#)] [[PubMed](#)]
10. Li, H.; Schopfer, L.M.; Nachon, F.; Froment, M.T.; Masson, P.; Lockridge, O. Aging Pathways for Organophosphate-Inhibited Human Butyrylcholinesterase, Including Novel Pathways for Isomalathion, Resolved by Mass Spectrometry. *Toxicol. Sci.* **2007**, *100*, 136–145. [[CrossRef](#)] [[PubMed](#)]
11. Kuca, K.; Musilek, K.; Jun, D.; Pohanka, M.; Zdarova-Karasova, J.; Novotny, L.; Musilova, L. Could oxime HI-6 really be considered as broad-spectrum antidote? *J. Appl. Biomed.* **2009**, *7*, 143–149.
12. De Koning, M.C.; Joosen, M.J.A.; Noort, D.; van Zuylen, A.; Tromp, M.C. Peripheral site ligand-oxime conjugates: A novel concept towards reactivation of nerve agent-inhibited human acetylcholinesterase. *Bioorg. Med. Chem.* **2011**, *19*, 588–594. [[CrossRef](#)] [[PubMed](#)]
13. Mercey, G.; Verdelet, T.; Saint-Andre, G.; Gillon, E.; Wagner, A.; Baati, R.; Jean, L.; Nachon, F.; Renard, P.Y. First efficient uncharged reactivators for the dephosphorylation of poisoned human acetylcholinesterase. *Chem. Commun.* **2011**, *47*, 5295–5297. [[CrossRef](#)] [[PubMed](#)]
14. Musilek, K.; Holas, O.; Jun, D.; Dohnal, V.; Gunn-Moore, F.; Opletalova, V.; Dolezal, M.; Kuca, K. Mono-oxime reactivators of acetylcholinesterase with (E)-but-2-ene linker—Preparation and reactivation of tabun- and paraoxon-inhibited acetylcholinesterase. *Bioorg. Med. Chem.* **2007**, *15*, 6733–6741. [[CrossRef](#)] [[PubMed](#)]
15. Musilek, K.; Komloova, M.; Holas, O.; Horova, A.; Pohanka, M.; Gunn-Moore, F.; Dohnal, V.; Dolezal, M.; Kuca, K. Mono-oxime bisquaternary acetylcholinesterase reactivators with prop-1,3-diyl linkage—Preparation, in vitro screening and molecular docking. *Bioorg. Med. Chem.* **2011**, *19*, 754–762. [[CrossRef](#)] [[PubMed](#)]
16. Kuca, K.; Kassa, J. A Comparison of the Ability of a New Bispyridinium Oxime—1-(4-hydroxyiminomethylpyridinium)-4-(4-carbamoylpyridinium)butane Dibromide and Currently used Oximes to Reactivate Nerve Agent-inhibited Rat Brain Acetylcholinesterase by In Vitro Methods. *J. Enzym. Inhib. Med. Chem.* **2003**, *18*, 529–535. [[CrossRef](#)] [[PubMed](#)]
17. Musilek, K.; Jun, D.; Cabal, J.; Kassa, J.; Gunn-Moore, F.; Kuca, K. Design of a Potent Reactivator of Tabun-Inhibited Acetylcholinesterase Synthesis and Evaluation of (E)-1-(4-Carbamoylpyridinium)-

- 4-(4-hydroxyiminomethylpyridinium)-but-2-ene Dibromide (K203). *J. Med. Chem.* **2007**, *50*, 5514–5518. [[CrossRef](#)] [[PubMed](#)]
18. Kuca, K.; Jun, D.; Musilek, K. Structural Requirements of Acetylcholinesterase Reactivators. *Mini Rev. Med. Chem.* **2006**, *6*, 269–277. [[CrossRef](#)] [[PubMed](#)]
  19. Kuca, K.; Cabal, J.; Musilek, K.; Jun, D.; Bajgar, J. Effective bisquaternary reactivators of tabun-inhibited AChE. *J. Appl. Toxicol.* **2005**, *25*, 491–495. [[CrossRef](#)] [[PubMed](#)]
  20. Lorke, D.E.; Nurulain, S.M.; Hasan, M.Y.; Kuca, K.; Musilek, K.; Petroianu, G.A. Eight new bispyridinium oximes in comparison with the conventional oximes pralidoxime and obidoxime: In vivo efficacy to protect from diisopropylfluorophosphate toxicity. *J. Appl. Toxicol.* **2008**, *28*, 920–928. [[CrossRef](#)] [[PubMed](#)]
  21. Sinko, G.; Brglez, J.; Kovarik, Z. Interactions of pyridinium oximes with acetylcholinesterase. *Chem. Biol. Interact.* **2010**, *187*, 172–176. [[CrossRef](#)] [[PubMed](#)]
  22. Pohanka, M.; Jun, D.; Kuca, K. Improvement of acetylcholinesterase-based assay for organophosphates in way of identification by reactivators. *Talanta* **2008**, *77*, 451–454. [[CrossRef](#)] [[PubMed](#)]
  23. Calic, M.; Vrdoljak, A.L.; Radic, M.; Jelic, D.; Jun, D.; Kuca, K.; Kovarik, Z. In vitro and in vivo evaluation of pyridinium oximes: Mode of interaction with acetylcholinesterase, effect on tabun- and soman-poisoned mice and their cytotoxicity. *Toxicology* **2006**, *219*, 85–96. [[CrossRef](#)] [[PubMed](#)]
  24. Kovarik, Z.; Vrdoljak, A.L.; Berend, S.; Katalinic, M.; Kuca, K.; Musilek, K.; Radic, B. Evaluation of oxime K203 as antidote in tabun poisoning. *Arh. Hig. Rada Toksikol.* **2009**, *60*, 19–26. [[CrossRef](#)] [[PubMed](#)]
  25. Tattersall, J.E.H. Ion channel blockade by oximes and recovery of diaphragm muscle from soman poisoning in vitro. *Brit. J. Pharmacol.* **1993**, *108*, 1006–1015. [[CrossRef](#)]
  26. Worek, F.; Aurbek, N.; Wille, T.; Eyer, P.; Thiermann, H. Kinetic analysis of interactions of paraoxon and oximes with human, Rhesus monkey, swine, rabbit, rat and guinea pig acetylcholinesterase. *Toxicol. Lett.* **2011**, *200*, 19–23. [[CrossRef](#)] [[PubMed](#)]
  27. Lorke, D.E.; Hasan, M.Y.; Arafat, K.; Kuca, K.; Musilek, K.; Schmitt, A.; Petroianu, G.A. In vitro oxime protection of human red blood cell acetylcholinesterase inhibited by diisopropyl-fluorophosphate. *J. Appl. Toxicol.* **2008**, *28*, 422–429. [[CrossRef](#)] [[PubMed](#)]
  28. Odzak, R.; Calic, M.; Hrenar, T.; Primožic, I.; Kovarik, Z. Evaluation of monoquaternary pyridinium oximes potency to reactivate tabun-inhibited human acetylcholinesterase. *Toxicology* **2007**, *233*, 85–96. [[CrossRef](#)] [[PubMed](#)]
  29. Musilek, K.; Holas, O.; Misik, J.; Pohanka, M.; Novotny, L.; Dohnal, V.; Opletalova, V.; Kuca, K. Monooxime-monocarbamoyl Bispyridinium Xylene-Linked Reactivators of Acetylcholinesterase—Synthesis, In vitro and Toxicity Evaluation, and Docking Studies. *ChemMedChem* **2010**, *5*, 247–254. [[CrossRef](#)] [[PubMed](#)]
  30. Worek, F.; Aurbek, N.; Thiermann, H. Reactivation of organophosphate-inhibited human AChE by combinations of obidoxime and HI 6 in vitro. *J. Appl. Toxicol.* **2007**, *27*, 582–588. [[CrossRef](#)] [[PubMed](#)]
  31. Kryger, G.; Harel, M.; Giles, K.; Toker, L.; Velan, B.; Lazar, A.; Kronman, C.; Barak, D.; Ariel, N.; Shafferman, A.; et al. Structures of recombinant native and E202Q mutant human acetylcholinesterase complexed with the snake-venom toxin fasciculin-II. *Acta Crystallogr. Sect. D* **2000**, *56*, 1385–1394. [[CrossRef](#)]
  32. Morris, G.M.; Goodsell, D.S.; Halliday, R.S.; Huey, R.; Hart, W.E.; Belew, R.K.; Olson, A.J. Automated docking using a Lamarckian genetic algorithm and an empirical binding free energy function. *J. Comput. Chem.* **1998**, *19*, 1639–1662. [[CrossRef](#)]
  33. Trott, O.; Olson, A.J. AutoDock Vina: Improving the speed and accuracy of docking with a new scoring function, efficient optimization, and multithreading. *J. Comput. Chem.* **2010**, *31*, 455–461. [[CrossRef](#)] [[PubMed](#)]
  34. Mercey, G.; Verdelet, T.; Renou, J.; Kliachyna, M.; Baati, R.; Nachon, F.; Jean, L.; Renard, P.-Y. Reactivators of acetylcholinesterase inhibited by organophosphorus nerve agents. *Acc. Chem. Res.* **2012**, *45*, 756–766. [[CrossRef](#)] [[PubMed](#)]
  35. Acharya, J.; Dubey, D.K.; Srivastava, A.K.; Raza, S.K. In vitro reactivation of sarin-inhibited human acetylcholinesterase (AChE) by bis-pyridinium oximes connected by xylene linkers. *Toxicol. In Vitro* **2011**, *25*, 251–256. [[CrossRef](#)] [[PubMed](#)]
  36. Musilek, K.; Dolezal, M.; Gunn-Moore, F.; Kuca, K. Design, evaluation and structure—Activity relationship studies of the AChE reactivators against organophosphorus pesticides. *Med. Res. Rev.* **2011**, *31*, 548–575. [[CrossRef](#)] [[PubMed](#)]

37. Musilek, K.; Roder, J.; Komloova, M.; Holas, O.; Hrabínova, M.; Pohanka, M.; Dohnal, V.; Opletalova, V.; Kuca, K.; Jung, Y.S. Preparation, in vitro screening and molecular modelling of symmetrical 4-tert-butylpyridinium cholinesterase inhibitors—Analogues of SAD-128. *Bioorg. Med. Chem. Lett.* **2011**, *21*, 150–154. [[CrossRef](#)] [[PubMed](#)]
38. Musilek, K.; Holas, O.; Kuca, K.; Jun, D.; Dohnal, V.; Dolezal, M. Synthesis of asymmetrical bispyridinium compounds bearing cyano-moiety and evaluation of their reactivation activity against tabun and paraoxon-inhibited acetylcholinesterase. *Bioorg. Med. Chem. Lett.* **2006**, *16*, 5673–5676. [[CrossRef](#)] [[PubMed](#)]
39. Kuca, K.; Jun, D.; Junova, L.; Musilek, K.; Hrabínova, M.; da Silva, J.A.V.; Ramalho, T.C.; Valko, M.; Wu, Q.; Nepovimova, E.; et al. Synthesis, Biological Evaluation, and Docking Studies of Novel Bisquaternary Aldoxime Reactivators on Acetylcholinesterase and Butyrylcholinesterase Inhibited by Paraoxon. *Molecules* **2018**, *23*, 1103. [[CrossRef](#)] [[PubMed](#)]
40. Pettersen, E.F.; Goddard, T.D.; Huang, C.C.; Couch, G.S.; Greenblatt, D.M.; Meng, E.C.; Ferrin, T.E. UCSF Chimera—A visualization system for exploratory research and analysis. *J. Comput. Chem.* **2004**, *25*, 1605–1612. [[CrossRef](#)] [[PubMed](#)]
41. DeLano, W.L. The PyMOL Molecular Graphics System. 2002. Available online: <http://www.pymol.org> (accessed on 6 September 2018).

**Sample Availability:** Samples of the compounds are available from the authors.



© 2018 by the authors. Licensee MDPI, Basel, Switzerland. This article is an open access article distributed under the terms and conditions of the Creative Commons Attribution (CC BY) license (<http://creativecommons.org/licenses/by/4.0/>).